A single point mutation in the LN domain of LAMA2 causes muscular dystrophy and peripheral amyelination

Bruce L. Patton[1], Bing Wang[2], Yukie S. Tarumi[1], Kevin L. Seburn[2] and Robert W. Burgess[2,*]

[1]Center for Research on Occupational and Environmental Toxicology, Oregon Health and Sciences University, Portland, OR 97239, USA
[2]The Jackson Laboratory, Bar Harbor, ME 04609, USA
*Author for correspondence (e-mail: Robert.burgess@jax.org)

Accepted 3 February 2008
Journal of Cell Science 121, 1593-1604 Published by The Company of Biologists 2008
doi:10.1242/jcs.015354

Summary

Mutations in the gene encoding the basal lamina (BL) component laminin α2 (*LAMA2*) cause merosin-deficient congenital muscular dystrophy 1A (MDC1A), a complex disorder that includes hypomyelination and myodegeneration. In *dystrophia muscularis* (*dy*) mice bearing *Lama2* mutations, myofibers and Schwann cells fail to assemble stable BLs, which are thought to be crucial for myofiber survival and Schwann cell differentiation. Here, we describe defects in a new allele of *Lama2* in mice, *nmf417*, in which a point mutation substitutes Arg for Cys79 at a universally conserved CxxC motif in the laminin N-terminal (LN) domain; this domain mediates laminin-laminin interactions. *nmf417* homozygosity caused progressive myodegeneration and severe peripheral amyelination in nerve roots, similar to previous *Lama2* mutations, but without the pervasive BL thinning previously associated with the disorder. In direct contrast to the previously characterized *dy* and *dy^{2J}* alleles, *nmf417* homozygous myofibers frequently had thickened BLs. Severe amyelination in *nmf417*-mutant nerve roots suggested complete laminin 2 inactivation for Schwann cells, although myelinated fibers had normal BLs. The results reveal crucial roles for the LN domain CxxC motif in both nerve and muscle, but challenge expected relationships between LN-domain function, Ln2 activity and BL stability. The *nmf417* mutation provides a defined animal model in which to investigate mechanisms and treatments for moderate forms of MDC1A.

Supplementary material available online at
http://jcs.biologists.org/cgi/content/full/121/10/1593/DC1

Key words: Merosin deficiency, Schwann cell, Myelination, Extracellular matrix, Assembly

Introduction

The surface of every muscle fiber and peripheral nerve fiber is covered by basal lamina (BL), a dense, mechanically stable sheet of extracellular matrix. The major glycoprotein in muscle and nerve BLs is laminin 2 (Lama2), also called merosin or LM-211 (Aumailley et al., 2005; Leivo and Engvall, 1988). Laminin 2 contains the α2, β1 and γ1 subunits, or chains, each encoded by a distinct gene. Laminin α2 mutations are the most common cause of early-onset muscular dystrophy (MDC1A) in humans (note: the human laminin α2 gene symbol is *LAMA2*), and cause a similar disorder in dogs and cats (Shelton and Engvall, 2005; Tome et al., 1994). However, disease mechanisms have been best studied in *Lama2*-mutant strains of mice, known as *dystrophia muscularis* (*dy*) mice (note: the mouse laminin α2 gene symbol is *Lama2*, but the mutation was first identified as *dy*) (Michelson et al., 1955; Miyagoe et al., 1997; Xu et al., 1994a; Xu et al., 1994b). Characteristically, dystrophy from *Lama2* is compounded by developmental defects in myelination, and BLs on muscle fibers and Schwann cells appear thin and discontinuous (Madrid et al., 1975; Nakagawa et al., 2001; Xu et al., 1994a). Accordingly, myofiber BLs are thought to provide a stable anchor for adhesion receptors in the sarcolemma and thus to absorb cytoskeletal stresses during movement. Similarly, Schwann cell BLs have been thought to orient Schwann cell growth and differentiation during myelination.

Biochemical, immunochemical, and genetic studies buttress this model. Laminins contain specific binding domains for receptors and for polymerization, and these occur in a polarized distribution that predisposes laminins to form sheet-like networks on cell surfaces. Laminins, like collagens, are composed of three extended polypeptides (α, β and γ chains) entwined cord-like over much of their length. However, the amino-halves of laminin chains are separated, forming 'short-arms' that branch from the main trunk. Globular 'LN' (laminin N-terminal) domains, one at the tip of each short arm, bind in a tripartite fashion to link laminin heterotrimers into extended networks. The carboxyl end of the trunk ends in a cluster of α-chain 'LG' (laminin G-like) domains, which control binding specificity for receptors such as integrins, dystroglycan and sulfatide. Thus, laminin biochemistry appears to be especially devoted to framing BLs (Colognato and Yurchenco, 2000).

In vivo and in vitro studies demonstrate that BL assembly requires at least one polymerizing laminin (Sasaki et al., 2004; Yurchenco et al., 2004a). Laminin 2 is the predominant isoform in nerve and muscle BLs, outside intercellular junctions (Patton et al., 1997). All *Lama2* mutations studied in mice disrupt BLs, and all laminin α2 mutations studied in humans and mice result in upregulation of the laminin α4 chain, expressed as laminin 8 (α4β1γ1) (Patton et al., 1999; Patton et al., 1997; Ringelmann et al., 1999). However, the α4 chain lacks the LN domain, and its upregulation is insufficient to sustain BL structure or prevent disease in *Lama2*-mutant mice,

further suggesting that loss of BL structure is pathogenic. By contrast, transgenic expression of the LN-containing α1 chain restores BL integrity, reduces myodegeneration and increases myelination in α2-mutant mice (Gawlik et al., 2004; Gawlik et al., 2006).

However, two prominent observations remain unexplained. First, the sarcolemma is reportedly stable in laminin-α2-mutant mice, in contrast with mice lacking dystrophin or the dystrophin-glycoprotein complex (DGC) (Straub and Campbell, 1997). The cytopathological mechanism is therefore unknown. Second, loss of BL structure might not account for differences in the severity of myodegeneration associated with *Lama2* mutations. For example, whereas *Lama2*-null mice (dy^{3K}) have severe dystrophy and die by 8 weeks, the dy^{2J} mutation, which causes an internal deletion in the α2 LN domain and disrupts BL integrity, causes moderate dystrophy and no mortality. Rescue studies confirm that mortality is due to dystrophy (Kuang et al., 1998). It is possible that the severity of dystrophy reflects the overall loss of laminin 2 protein affected by specific mutations, with myodegeneration varying primarily from progressive loss of BL stability. Alternatively, laminin 2 might act through multiple mechanisms that are selectively inactivated by specific mutations. These questions are directly relevant to human MDC1A, in which complete *LAMA2* deficiency is associated with perinatal onset and death in adolescence, whereas mutations that leave C-terminal portions of α2 intact are associated with distinctly milder dystrophy (Cohn et al., 1998; Sewry et al., 1997).

In contrast to muscle, all mouse *Lama2* mutations similarly disrupt peripheral myelination (Biscoe et al., 1975; Bradley and Jenkison, 1973; Nakagawa et al., 2001; Weinberg et al., 1975). Immature Schwann cells lacking laminin 2 fail to proliferate and differentiate properly during the perinatal process of axonal (radial) sorting. As a result, nerves in *dy*-strain adults contain large bundles of 'amyelinated' axons. Myelination in spinal roots is almost entirely dependent on laminin 2, whereas myelination in distal nerves is more equally dependent on laminin 2 and laminin 8, making the ventral roots a sensitive indicator of laminin 2 function in myelination (Yang et al., 2005). Loss of BL structure on Schwann cells lacking α2 was initially thought to be responsible for amyelination (Bunge et al., 1986; Madrid et al., 1975). However, considerable evidence now argues that BL formation per se is not germane (Nakagawa et al., 2001; Yang et al., 2005). Nevertheless, the dy^{2J} deletion of the α2 LN domain almost completely inactivates the ability of laminin 2 to promote myelination. We have suggested that laminin 2 polymerization mediated by the LN domain is required to foster receptor aggregation over short distances, rather than BL formation (Yang et al., 2005). Alternatively, the α2 LN domain might have a specific receptor-mediated function in promoting myelination, or amyelination in dy^{2J} mice might result from reducing laminin 2 levels below a critical threshold (Sunada et al., 1995; Xu et al., 1994b).

Here, we identify a *Lama2* point mutation in *nmf417* mice that causes muscular dystrophy and amyelination similar to *dy* and dy^{2J}, but without loss of laminin 2 expression or BL stability previously associated with the disorder. The mutation changed Cys79 to Arg, thereby disrupting a paired cysteine motif (CxxC) conserved in all known laminin LN domains, both vertebrate and invertebrate. These findings suggest that the widely held hypothesis that laminin 2 promotes myelination and prevents dystrophy primarily through its role in maintaining BL stability is overly simplistic. Observations in *nmf417* nerves demonstrate a role for the LN domain of α2 that is separate from overall laminin 2 expression, and suggest that additional factors play major roles in modulating BL stability.

Results

A program of chemical mutagenesis at The Jackson Laboratory, designed to identify genetic causes of neurological disease in mice, isolated a heritable recessive mutation, *nmf417*, resulting in overt neuromuscular dysfunction. In initial litters from unaffected parents, four of 21 offspring developed general skeletal muscle wasting at juvenile ages and bilateral contractures of the hind limbs as young adults. Preliminary histological examination of muscles at 8 weeks found hallmarks of muscular dystrophy, including widespread endomysial fibrosis, focal necrosis and central nuclei typical of regenerated fibers. In addition, sections through the spine revealed severe hypomyelination in nerve roots, but not in spinal cord. Combined skeletal muscular dystrophy and peripheral hypomyelination is consistent with the phenotype of *dy*, which results from loss-of-function mutations in *Lama2* (Sunada et al., 1995; Xu et al., 1994b). We tested for genetic non-complementation by mating mice known to be heterozygous for the *nmf417* and $Lama2^{dy}$ (*dy*) mutations. Three of ten offspring were dystrophic, indicating that *nmf417* is a *Lama2* allele.

To confirm and identify a *Lama2* mutation, the entire open reading frame of cDNA generated from an affected *nmf417* mouse was sequenced and compared with isogenic C57BL/6J sequence. Consistent with ethylnitrosourea (ENU)-induced mutations, a single base change from T to C was found at the first position of codon 79, which converts Cys79 to Arg (Fig. 1A-C). Primer-mismatch PCR based on this mutation gave specific but distinct bands in *nmf417* and wild-type mice, and was used for subsequent genotyping (see Materials and Methods and supplementary material Fig. S1). There were no other coding-sequence differences between isogenic control C57BL/6J and *nmf417*. Using cDNA prepared from heterozygous mice, chromatogram peaks of nearly equal intensity were observed for both T and C, suggesting that wild-type and *nmf417 Lama2* mRNA transcripts are similarly stable in vivo (Fig. 1B).

Cys79 (C79) is conserved in all known LAMA2 sequences, including mammals, birds, and the *Drosophila* and *Caenorhabditis elegans* orthologs (Fig. 1D,E). Within the α2 chain, Cys79 is centered in the LN domain at the free end of the short arm (Fig. 1F), which is implicated in mediating laminin-laminin interactions and BL assembly (Cheng et al., 1997; Yurchenco, 1990). The previously described dy^{2J} allele of mouse *Lama2* generates an internal deletion within the LN domain that includes C79 and disrupts laminin 2 polymerization and BL formation (Sunada et al., 1995; Xu et al., 1994b; Colognato and Yurchenco, 1999). Therefore, the C79R mutation in *nmf417* might identify a key residue for promoting BL formation. Alternatively, the C79R mutation could decrease overall laminin 2 expression or stability, or act by disrupting LN domain activities unrelated to BL formation. To distinguish these possibilities, we assessed the severity of the *nmf417* allele, determined levels of laminin 2 protein expression in *nmf417*, and assessed whether myodegeneration and dysmyelination had a similar relationship to BL structure as that observed in other *Lama2* alleles (Table 1).

nmf417 behaves as a partial loss-of-function allele

We assessed general disease progression in *nmf417* homozygous mice. The body weight of *nmf417* homozygotes did not significantly diverge from control values until the fifth week (supplementary

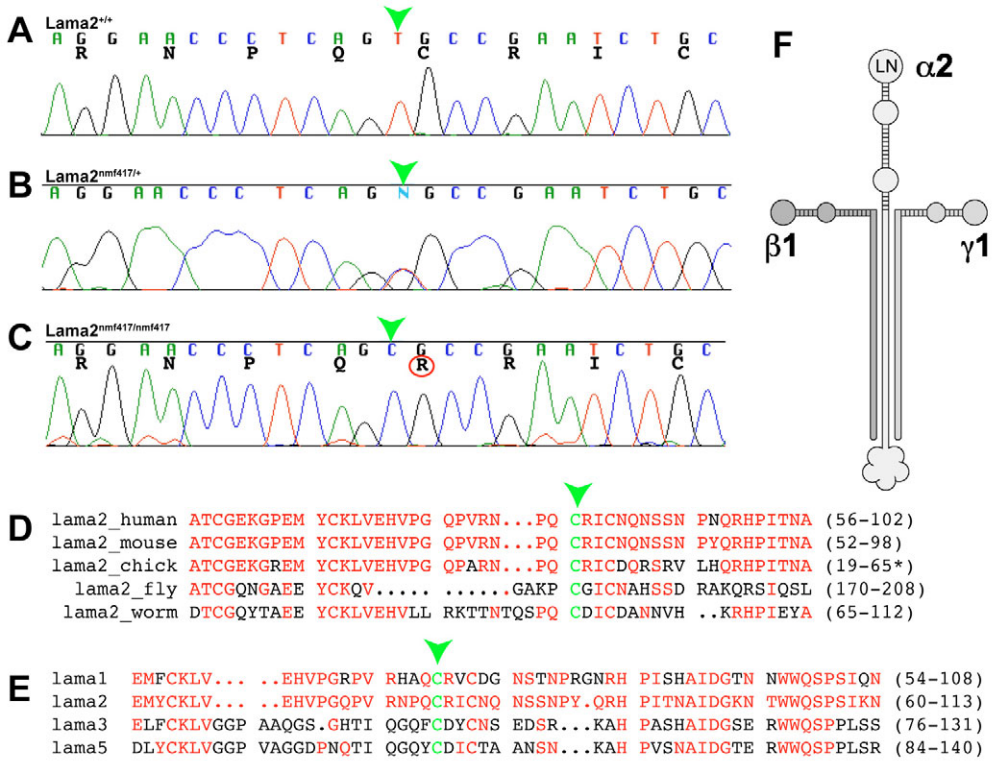

Fig. 1. The *Lama2*^{nmf417} mutation. (A-C) cDNA-sequence chromatograms from (A) wild-type, (B) heterozygous mutant *nmf417* and (C) homozygous mutant *nmf417* mice revealed mutation of T to C in the first position of codon 79 (arrowheads), which changes Cys79 to Arg (circled residue in C). Translation is shown above each chromatogram. (B) Intensities of the C- and T-containing sequences were similar in *nmf417* heterozygotes, suggesting that the two transcripts were similarly abundant. (D) Alignment of laminin α2 peptide sequences from human, mouse and chicken, and their homologs in *Drosophila* and *C. elegans*, reveals phylogenetic conservation of Cys at this position (arrowhead). Residues identical to mouse are shown in red; peptide positions are shown at the right, provisional for the incomplete chick sequence (*). (E) Cys79 in α2 is conserved in all laminin α chains containing an LN domain. (F) Laminin 2 is a heterotrimer of the α2, β1 and γ1 orthologs, with N-terminal portions separated and C-terminal portions entwined in a coiled-coil. LN domains at each N-terminus mediate aggregation. The α chain ends in a series of LG domains, which bind to cell receptors. The *nmf417* mutation is in the α2 LN domain.

material Fig. S2, $P<0.01$ at 5 weeks). This is markedly later than *dy*^{w} or *dy*^{3K} homozygous mice, which show reduced size by 2 weeks of age, but is earlier than *dy*^{2J} homozygotes, in which growth is not strongly affected (Kuang et al., 1998; Miyagoe et al., 1997; Moll et al., 2001). The *nmf417* homozygotes showed no mortality by 6 months, and bred and reared litters efficiently. However, their movements became visibly impaired by weaning, and hindlimbs became partially paralyzed by 6 weeks of age, although some hindlimb function was retained at 8-10 months. Mice homozygous for severe *Lama2* alleles such as *dy*^{3K} or *dy*^{W} become cachexic and die by 8-12 weeks, whereas mice homozygous for the original *dy* allele rarely breed, develop permanent hindlimb contractures at 10-12 weeks of age and most die by 6 months. Mice homozygous for the *dy*^{2J} allele have permanent contractures by 12 weeks, but are fertile and do not have a shortened lifespan. Thus, the overt phenotype of *nmf417* homozygotes is most similar to mice homozygous for the *dy*^{2J} allele, although the *nmf417* growth rate was more impacted. Interestingly, however, *nmf417* hindlimb paralysis was also less severe than that of *dy*^{2J} homozygous mice, suggesting partially divergent phenotypes for the *nmf417* mutation and *dy*^{2J} internal deletion in nerve and muscle.

Laminin α2 protein in *nmf417* muscle

We next assessed laminin 2 production in muscle and nerve using antibodies specific to the α2 chain. Consistent with the milder phenotype of the homozygous mice, the intensity of immunoreactivity for α2 in cryostat sections of adult *nmf417/nmf417* muscles was similar to age-matched littermate

Table 1. *Lama2* alleles in mouse

Allele	Mutation	Effect on protein	Reference
dy	Unknown	Reduced protein levels in muscle, severely reduced in nerve, wild-type sequence	(Michelson et al., 1955; Xu et al., 1994a; Sunada et al., 1994)
dy^{2J}	Splicing, skips exon 2	57 amino acid deletion in the LN domain, reduced protein levels	(Xu et al., 1994b; Sunada et al., 1995)
dy^{W}	Targeted	Very low abundance, truncated protein	(Kuang et al., 1998)
dy^{3K}	Targeted	Null	(Miyagoe et al., 1997)
dy^{nmf417}	ENU point mutation	C79 to R, normal levels and localization	This report

The alleles of the *Lama2* gene in mice, their genetic lesion, effect on the LAMA2 protein and references are provided.

controls, and α2 was co-concentrated with β1 and γ1 chains along myofiber surfaces, and was generally absent inside myofibers and between fibers (Fig. 2A-F). Similar results were obtained with antibodies directed against the short arms and LG domains of α2, and in fixed and unfixed tissues (not shown). The results suggested that the C79R mutant α2 chain is correctly synthesized and assembled into laminin 2 heterotrimers, secreted and, stably incorporated into myofiber surface matrix. To verify these conclusions, we prepared sarcolemma fractions from leg muscles of *nmf417/nmf417* and control mice, separated insoluble matrix proteins from other membrane-associated proteins by detergent extraction, and immunoblotted under non-reducing conditions to preserve the chain linkage within laminins. Blots revealed stable matrix incorporation and co-migration of C79R α2 chain with β and γ chains at normal heterotrimer mobilities (Fig. 2G). The abundance of α2 in mutant muscle was determined by western blotting directly from tissue homogenates using denaturing and reducing conditions (Fig. 2H). The primary band detected in both *nmf417/nmf417* and control samples migrated at the expected size of 320 kDa for the major α2 fragment. Lanes were loaded with equal amounts of sample protein (20 μg) and signal intensities were standardized for loading variation by re-probing blots with an antibody against myosin heavy chain. Using this standard, the mutant samples showed an increase in laminin α2 abundance (142±22% of control, mean ± s.e. in analysis of eight mutant and seven control lanes prepared from four *nmf417/nmf417* and four control samples, 8-9 weeks of age). This apparent increase might partly reflect a loss of myosin in the dystrophic muscles, but indicates that there is no decrease in α2 levels below a critical threshold in the *nmf417/nmf417* muscle. Thus, the C79R mutation does not significantly affect α2-chain size, stability, heterotrimer assembly, basement membrane incorporation or abundance. The normal mobility of *nmf417* laminin 2 also suggests that glycosylation is not affected by the C79R mutation. The *nmf417* allele, therefore, contrasts with the *dy* and dy^{W} mutations, which substantially reduce laminin 2 levels in myofiber BLs, and dy^{3K}, which eliminates it.

At neuromuscular junctions (NMJs), identified by α-bungarotoxin staining for acetylcholine receptors, the α2 chain is assembled in trimers with the β2 chain as laminin 4 (α2β2γ1) (Patton

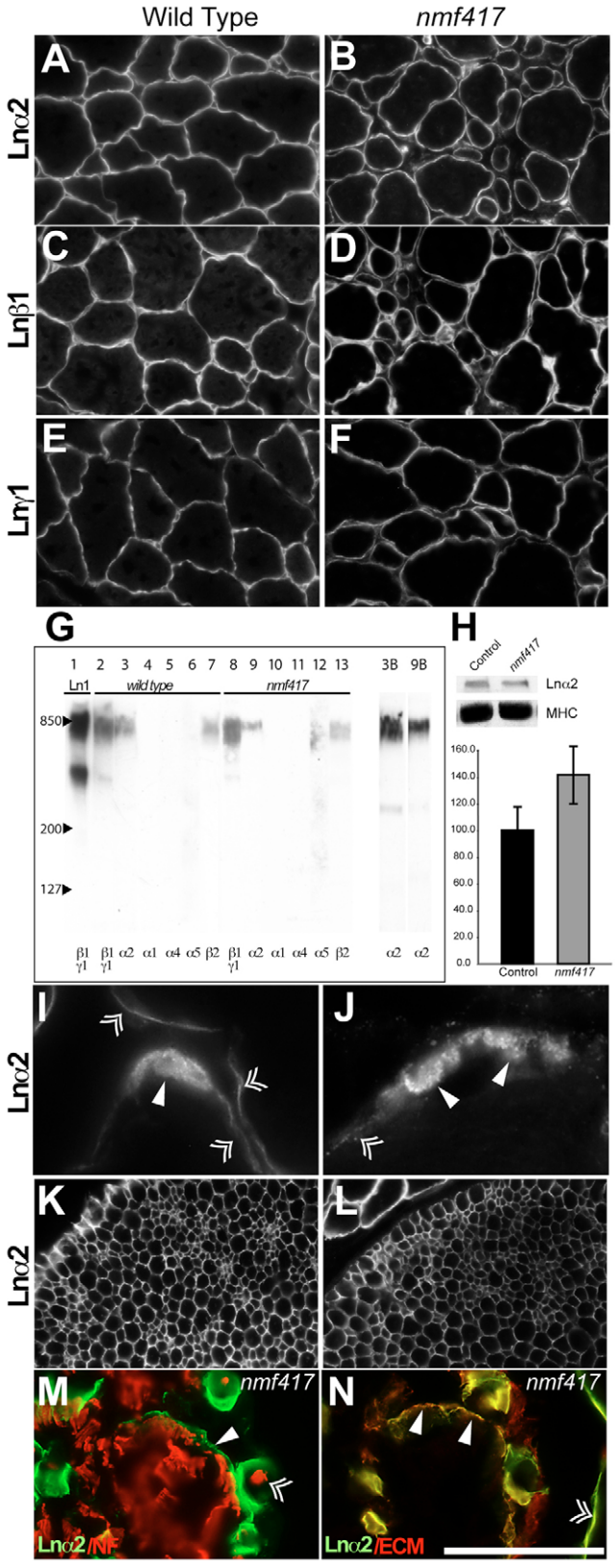

Fig. 2. Laminin 2 association with *nmf417* sarcolemma. (A-F) Cross-sections of quadriceps immunostained with antibodies against laminin α2, β1 and γ1. These concentrated at similar levels in both normal and *nmf417* homozygotes. Samples were stained in parallel and imaged with identical settings. (G) Immunoblotting of non-reduced BL-enriched matrix fractions from control and *nmf417* muscles showed co-migration of α2, β1 and γ1 at similar heterotrimer mobilities, and at similar relative abundance. Control and mutant samples contained equal total-protein content. Longer exposures (lanes 3B, 9B) showed no appreciable degradation of α2 in *nmf417* muscle. α1- and α4-laminins were not significantly upregulated in *nmf417* matrix. Variable immunoreactivity for α5 was noted in *nmf417* samples (lane 12), but without a distinct band pattern and without corroboration by immunostaining beyond its normal distribution in blood vessels (see Fig. 8F). Reactivity for laminin β2, which did not change, probably reflects vascular BLs. Laminin 1 (Ln1), purified α1β1γ1 protein. Values at left indicate relative molecular mass. (H) Reducing western blots on crude muscle homogenates indicated that α2 levels were not decreased in *nmf417/nmf417* mutant muscle. The myosin heavy chain was used as a control. (I,J) Laminin α2 is enriched at the NMJ (arrowheads) over extrasynaptic regions (double arrows) in both control (I) and *nmf417*-homozygous (J) samples. (K,L) Medial sciatic nerve sections stained for α2 show similar expression by wild-type (K) and *nmf417* (L) Schwann cells. (M) In *nmf417/nmf417* nerves, laminin-α2-positive immature Schwann cells (green) enwrap bundles of unmyelinated axons (arrowhead), whereas strong laminin α2 immunoreactivity is detected in the BL of myelinated axons (double arrow; laminin α2 in green, neurofilament in red). (N) Laminin α2 (green) colocalizes with other laminin 2 chains (β1 and γ1) and with nidogen on immature Schwann cells (arrowheads). The muscle BL is noted (double arrowhead). Scale bar: 60 μm (A-F,K,L); 15 μm (I,J,M,N).

et al., 1997; Sanes et al., 1990). We found that synaptic BLs at *nmf417/nmf417* NMJs contained normal levels of the α2 and β2 chains, indicating normal assembly and targeting of laminin 4, as well as of other synaptic extracellular matrix components (Fig. 2I,J and supplementary material Fig. S3). Laminin 4 also replaced laminin 2 at *nmf417* myotendinous junctions, as in normal muscle (not shown). These results are in contrast to those from *dy* muscles, in which the α2 chain is selectively absent from synaptic BLs, while low levels of laminin 2 persist in extrasynaptic BLs (Patton et al., 1997; Sewry et al., 1998).

Laminin α2 protein in *nmf417* nerves

Previous α2 mutations diminish laminin 2 levels in nerves more than in muscles. Laminin 2 is undetectable on Schwann cells in *dy*, dy^{W} or dy^{3K} homozygous mice (Gawlik et al., 2006; Nakagawa et al., 2001; Patton et al., 1997; Sewry et al., 1998; Sunada et al., 1994). In dy^{2J} homozygotes, laminin 2 levels on Schwann cells are decreased and what remains is distributed in a granular pattern, consistent with disruption of endoneurial BL structure observed by transmission electron microscopy (TEM) (Yang et al., 2005). By contrast, we found no quantitative decrease or qualitative disruption in the distribution of the mutant α2 chain in *nmf417/nmf417* sciatic nerves compared to littermate controls (Fig. 2K,L). Qualitatively similar results were observed in *nmf417/nmf417* spinal roots. Immature Schwann cells on the surface of axon bundles expressed laminin α2 with other BL components, including laminin β1, γ1 and nidogen (Fig. 2M,N). Thus, in nerve, as in muscle, the α2 C79R mutation had little or no effect on the secretion or incorporation of laminin 2 into the cell surface matrix. The C79R mutation is unique in separating loss of a specific α2 function from more general effects on laminin 2 expression or cell-surface-receptor interactions manifested in other *dy*-mutant strains.

Dystrophy and amyelination

Muscle and nerve structure were assessed at young adult ages (7-8 weeks). In normal muscles, myofibers generally had similar diameters, were closely associated with neighboring fibers and had myonuclei located immediately beneath the sarcolemma (Fig. 3A). In *nmf417/nmf417* muscles, the myofiber population included small as well as large caliber fibers separated by monocyte-rich endomysial connective tissue, and many contained centrally located nuclei (Fig. 3B), which mark fibers that have regenerated postnatally in place of original embryo-derived fibers. Qualitatively similar defects were present in all homozygous *nmf417* mice examined, in axial as well as limb muscles, and in muscles composed of predominantly fast fibers (plantaris, Fig. 3) and slow fibers (soleus, supplementary material Fig. S4). In direct comparisons, dystrophic changes in *nmf417* mice were comparable to dy^{2J} mice and less severe than *dy* (Fig. 3C,D) [*n*=5 *nmf417*, 4 dy^{2J}, 3 *dy* homozygotes, and >10 littermate control mice examined; all at postnatal day (P)59]. The regenerative capacity of *nmf417/nmf417* plantaris muscle was also assessed in these samples by counting overall fiber number and the percentage of central nuclei (supplementary material Fig. S5). In both *nmf417* and dy^{2J} homozygotes, muscle-fiber number was not significantly decreased and a similar percentage of fibers showed central nuclei, an indicator of regeneration. By contrast, *dy* homozygotes showed reduced fiber number and a trend towards a lower percentage of fibers with central nuclei, indicating more-severely impaired regenerative capacity in the *dy* allele than in *nmf417* or dy^{2J}. Thus, in all regards, the level of myodegeneration in *nmf417* homozygotes was consistent with the less severe overt phenotype of this allele.

We assessed myelination in the spinal roots, in which axonal sorting is almost completely dependent on laminin 2. Defects in axonal sorting preserve embryonic organization, with immature Schwann cells bordering large 'amyelinated' axon fascicles, and this defect is thus readily distinguished from demyelinating neuropathy. All previously reported *Lama2* mutations cause severe amyelination in spinal roots. Similarly, we found that most axons in *nmf417/nmf417* roots lacked ensheathing processes of Schwann-cells and were grouped in large bundles (Fig. 4A-D). Electron microscopy confirmed that axons in bundles were generally devoid of Schwann cell processes (Fig. 4F-G), as described in *dy* and dy^{2J} mice (Bradley and Jenkison, 1973; Bradley and Jenkison, 1975; Weinberg et al., 1975). The number and distribution of myelinated axons in *nmf417* roots was similar to *dy* and dy^{2J} roots (*n*=4 *nmf417*,

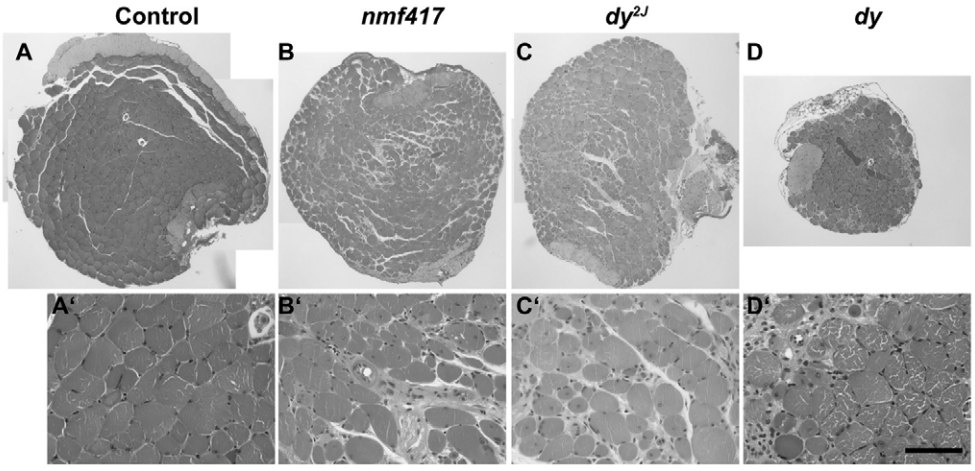

Fig. 3. Muscle pathology in *Lama2* mutants. (A-D′) Low (A-D) and high (A′-D′)-magnification images of age-matched (P59) plantaris muscles stained with H&E. (A) Normal muscle fibers were closely aligned, had a narrow distribution of calibers and contained peripheral nuclei. (B) In *nmf417*-homozygote muscles, the myofiber population contained many smaller fibers, which were interposed by endomysial connective tissue and monocyte-rich lesions, and many fibers contained central nuclei. (C) Dystrophic changes in dy^{2J} muscle were comparable to those in *nmf417* muscle. (D) Dystrophic changes in *dy*-homozygote muscle were more severe than in *nmf417*, including increased fiber loss and fibrotic lesions. Scale bar: 300 μm (A-D); 75 μm (A′-D′).

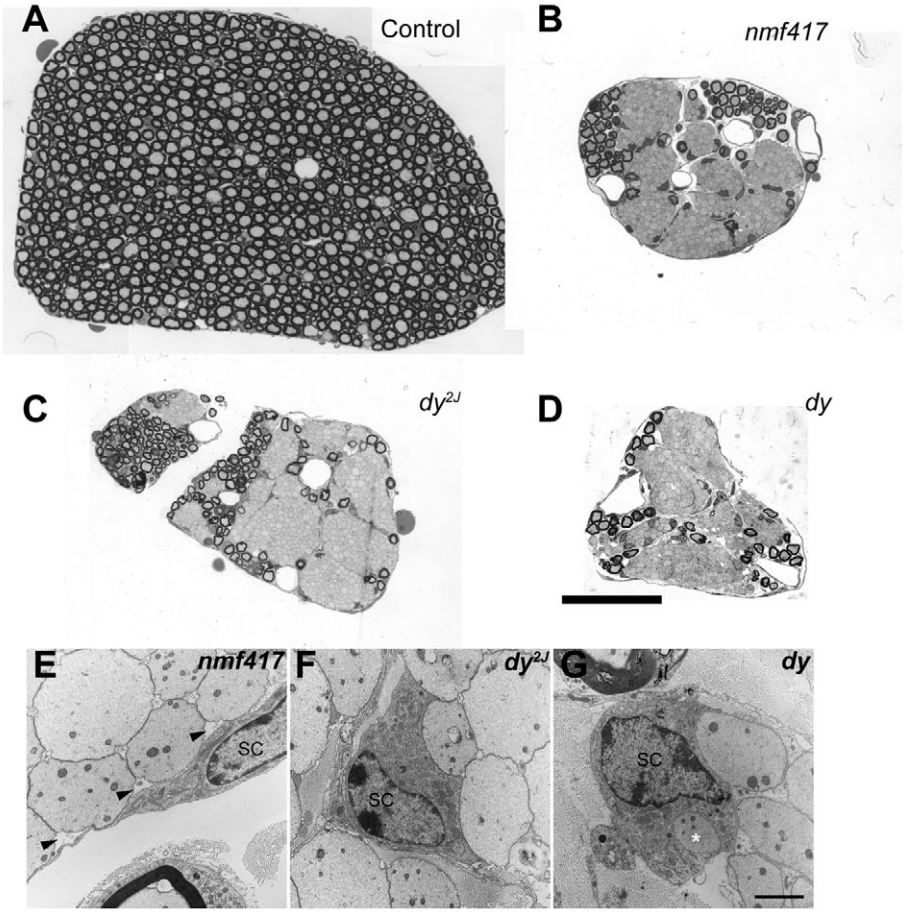

Fig. 4. Amyelination in *Lama2* mutants. Resin sections of the fifth lumbar ventral root taken at P59 were stained with Toluidine Blue to assess myelination (dark rings) of motor axons. (A) All motor axons are separated and uniformly myelinated in normal mice. (B) In *nmf417* homozygotes, myelinated axons are largely replaced by bundles of unmyelinated axons. Immature Schwann cells associated with bundle surfaces. Defects in myelination in *nmf417/nmf417* were similar in form and degree to that observed in homozygotes for the dy^{2J} allele (C) and the *dy* allele (D). (E) In *nmf417*, premyelinating Schwann cells (SC) were only loosely associated with axons (arrowheads) and were not invasive. (F) In dy^{2J}, premyelinating Schwann cells associated more tightly with axon bundles than in *nmf417.* (G) Premyelinating Schwann cells in *dy* mutants had tight axon associations, similar to dy^{2J}. Invasive processes were sometimes observed to engulf an axon in *dy* (asterisk) and dy^{2J} mutants without proceeding to myelination. All images show spinal ventral roots. Scale bars: 72 μm (A-D); 2 μm (E-G).

4 dy^{2J}, 6 *dy* homozygous mice; age 59 days for the *nmf417* and dy^{2J}, 5-9 months for *dy*; >10 littermate controls were examined). Thus, the *dy*, dy^{2J} and *nmf417* mutations result in similarly severe forms of amyelination. Previous work indicates the internally deleted laminin 2 of dy^{2J} is essentially inactive for myelination, because residual myelination is completely dependent on laminin 8 (Yang et al., 2005). The phenotypic similarity suggests that the *nmf417* α2-C79R mutation also inactivates laminin 2 for myelination.

We noted two differences in the axon–Schwann-cell relationship between *nmf417*, *dy* and dy^{2J} mutants. First, the extent of amyelination phenotype was consistent in *nmf417/nmf417* mice but varied in dy^{2J} homozygotes (supplementary material Fig. S6). Second, the immature Schwann cells on the surface of bundles in *nmf417* homozygotes typically adhered loosely to axons, and did not extend processes into bundles (Fig. 4E), a phenotype reminiscent of mice lacking Rac1 (Benninger et al., 2007; Nodari et al., 2007). By contrast, immature Schwann cells along *dy* and dy^{2J} bundles were tightly associated with axons, and often extended invasive processes into bundles, albeit without completing myelination (Fig. 4F,G) (*n*=4 *nmf417/nmf417* mice, 4 dy^{2J}/dy^{2J} mice and 3 *dy/dy* mice; four littermate controls of the *nmf417* mice were examined in nerve TEM studies; all mice were P59 except *dy/dy* which were 218±64 days old).

These data extend observations in dy^{2J}/dy^{2J} sciatic nerves (Yang et al., 2005) to suggest that Schwann cells in dy^{2J}/dy^{2J} roots retain a limited capacity to initiate radial sorting, but that progress towards myelination is highly susceptible to interruption. The dy^{2J} mutation causes a splicing defect that results in exon 2 being skipped. Variability in dy^{2J}/dy^{2J} roots could derive in part from variable efficiency of splicing between cells. Regardless, Schwann cells in *nmf417/nmf417* roots appeared comparatively inactive even at the earliest steps of radial sorting.

BL structure

Laminin-α2-related dystrophy and amyelination are associated with defects in BL formation (Madrid et al., 1975; Moll et al., 2001; Xu et al., 1994a). Using TEM, BLs are seen to consist of two main layers: the relatively unstained lamina rara immediately adjacent to the plasma membrane, and the heavily stained lamina densa (Fig. 5A). Consistent with previous reports, the lamina densa on muscle fibers in *dy* mutants was typically discontinuous, sparse and enmeshed with collagen fibrils from the collapse of the outer reticular lamina onto the plasma membrane (Fig. 5B). Unexpectedly, myofibers in *nmf417* muscles possessed a continuous lamina densa that lacked collagen fibrils and was typically thicker than controls (Fig. 5C). Essentially identical results were observed in all muscle examined in each cohort (*n*=5 *nmf417* mice, 3 *dy* mice, and 7 littermate controls, all P59).

We next investigated whether *nmf417* Schwann cells also assembled BLs. In mammals, Schwann cells in contact with axons form BLs containing a continuous lamina densa that separates the abaxonal plasma membrane from the collagen-rich interstitial matrix (Fig. 6A). In direct comparisons, we found that Schwann

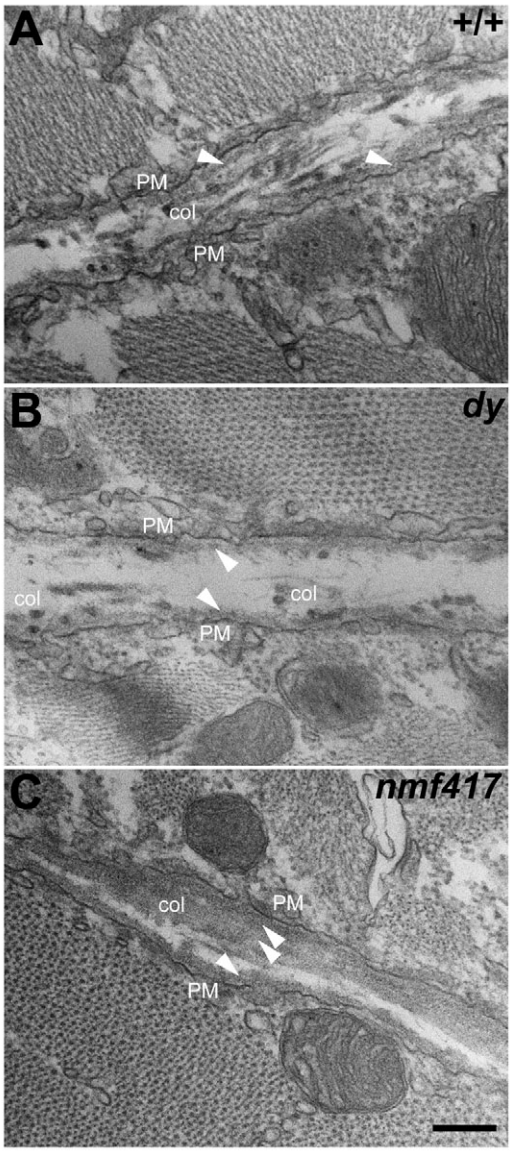

Fig. 5. Ultrastructure of muscle BLs. (A) In metal-stained ultrathin sections, myofiber membranes in wild-type mice are covered by a continuous BL, consisting of a transparent lamina rara adjacent to the plasma membrane (PM), a lamina densa (arrowheads) and an external reticular lamina that is rich in collagen fibrils (col). (B) In *dy* homozygotes, the BL is typically collapsed, with a thin lamina densa enmeshed with collagen fibrils adjacent to the sarcolemma. (C) In *nmf417*, myofiber BLs retain a layered structure, although the lamina densa is often thicker than normal. Scale bar: 200 nm.

cell BLs in dy^{2J} mice had a discontinuous lamina densa, and *dy* Schwann cells had very sparse BLs (Fig. 6B,C), consistent with levels of laminin 2 protein in these nerves. Interestingly, in *nmf417* homozygotes, all myelinating Schwann cells possessed intact BLs that were indistinguishable from wild type (Fig. 6D). However, all non-myelinating Schwann cells in *nmf417* mice (including premyelinating cells bordering amyelinated axons) lacked BLs entirely, similar to their counterparts in *dy* and dy^{2J} mice (Fig. 6E-G). Laminin 2 was expressed on premyelinating Schwann cells in *nmf417* mice (Fig. 2M,N) but, despite its presence, these cells do not form a compact BL that is visible by TEM. Therefore, the C79R mutation does compromise the ability of laminin 2 to organize BLs on a subset of cell types. Importantly, the inability of the *nmf417* mutant form of laminin 2 to establish stable interactions on immature Schwann cells brings the C79R mutation into line with previous interpretations regarding the mechanisms of laminin 2 in myelination (Yang et al., 2005). However, it also raises the issue of why the C79R mutation does not disrupt BL formation on myelinating Schwann cells, or on myofibers. BL stability is evidently modulated by additional factors that are differentially expressed by myelinating and non-myelinating Schwann cells.

BL composition

Primary BL components other than laminins, including type IV collagens, nidogen and perlecan, were present at normal levels in *nmf417* nerve and muscle as were the primary laminin receptors, the DGC and β1-integrins (Figs 7, 8). Combined with TEM (Figs 5, 6), these results indicate that the extracellular matrix of *nmf417* muscle fiber contains an intact basement membrane of normal composition. Although alternative laminin α-chains containing an LN domain were primary candidates to maintain BL stability in *nmf417* mice, we found no compensatory upregulation of α1, α3 or α5 (n=5 mutant and littermate controls each, at age 59 days). Interestingly, however, only a minority of myofibers in *nmf417* mice expressed elevated levels of laminin α4. This result is unique among *Lama2* alleles. Two manipulations reliably increase α4 expression: muscle injury leads to re-expression of α4 by immature regenerating myofibers (Patton et al., 1999), and all previously studied α2 mutations in mice and human MDC1A have been accompanied by marked and uniform increases in α4 laminin on both mature myofibers and myelinating Schwann cells (Nakagawa et al., 2001; Patton et al., 1999; Patton et al., 1997; Ringelmann et al., 1999). The ability of the α4 protein to compensate for the *nmf417* mutation is doubtful, because α4 lacks the N-terminal LN domain. In normal development, α4 laminins are highly expressed by immature Schwann cells and myofibers (Patton et al., 1997), and are then downregulated perinatally (Ringelmann et al., 1999). In adults, α4 is normally undetectable in extrasynaptic myofiber BLs and low on myelinating Schwann cells, but remains high on non-myelinating Schwann cells (Patton et al., 1997; Previtali et al., 2003; Yang et al., 2005). The limited upregulation of α4 in *nmf417* muscle is most consistent with transient expression by regenerating fibers. Thus, *nmf417* is unique for not expressing α4 laminins on Schwann cells and myofibers in response to a loss-of-function α2 mutation. Of particular interest, we noted that high laminin α4 expression therefore correlates directly with loss of BL stability in *nmf417*, and also dy^{2J}, mice.

Discussion

The results of the study of the $Lama2^{nmf417}$ allele allow us to draw several mechanistic conclusions. First, C79 in the CxxC motif of the laminin α2 chain is very specifically affected in the *nmf417* allele, demonstrating it to be crucial for the onset of myelination by Schwann cells in spinal roots and for the stability of mature skeletal muscle fibers. The CxxC motif is invariant among laminin LN domains, and is shared by other LN-domain proteins, such as netrin, but its function has not previously been tested. Second, the resulting dystrophy and amyelination are not caused by decreased laminin α2 abundance, either through inefficient translation or instability; nor are they caused by protein mislocalization, a failure to assemble laminin trimers or by detectable changes in the composition of the extracellular matrix. Third, the C79R mutation does not disrupt the ultrastructural integrity of the BL on myelinating

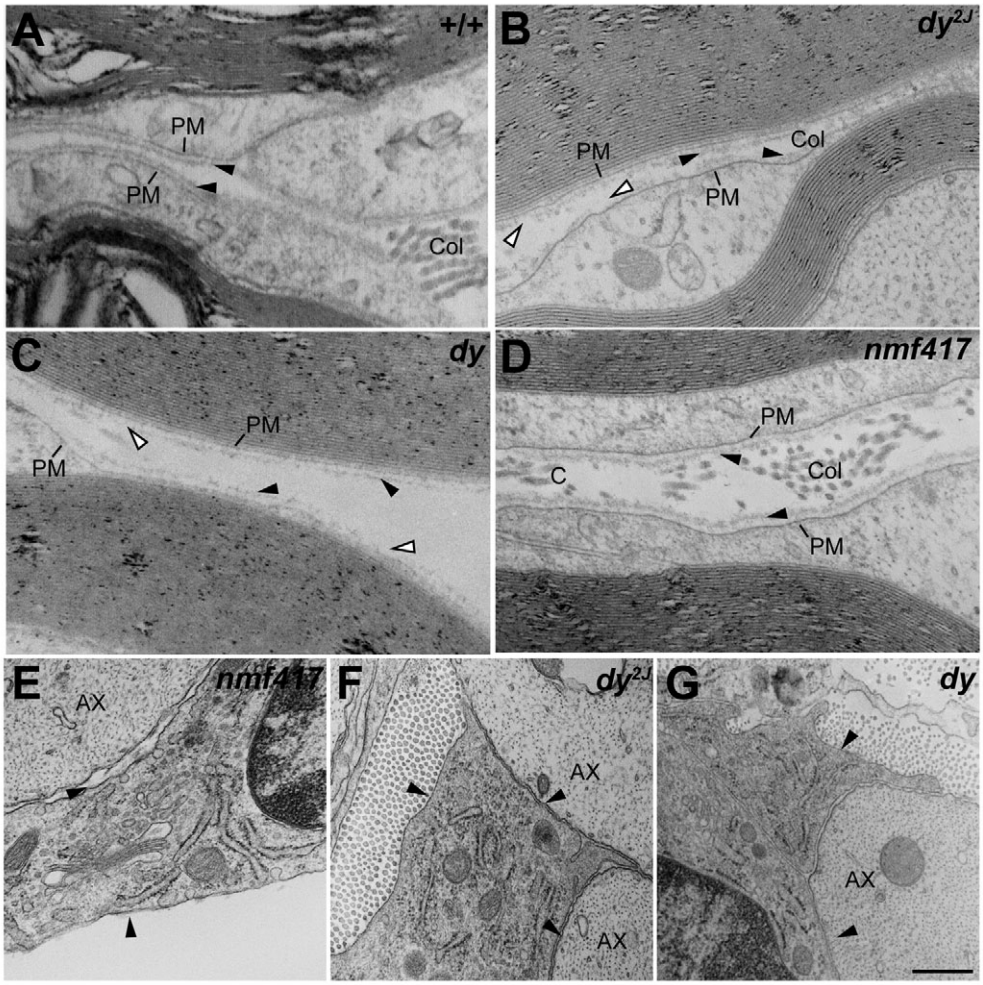

Fig. 6. Schwann cell BL formation and axon interactions in α2 mutants. (A) Normal Schwann cells form continuous BLs (arrowheads) adjacent to the plasma membrane (PM), with collagen fibrils between cells (Col). (B) In *dy*^{2J}, BLs on myelinating cells contained gaps (white arrowheads) and were comparatively indistinct. (C) In *dy*, myelinating Schwann cell BL is very sparse (black arrowheads) and discontinuous. (D) In *nmf417*, BLs on myelinating Schwann cells were continuous (arrowheads), but less compact. (E) BLs were absent from premyelinating Schwann cells in *nmf417* (arrowheads). AX, axons. (F) In *dy*^{2J}, premyelinating Schwann cells also lacked BLs. (G) Premyelinating Schwann cells in *dy* also lacked BLs (arrowheads). All images show L5 ventral roots. Scale bar: 250 nm (A-D); 500 nm (E-G).

Schwann cells and muscle fibers. Each of these conclusions is distinct from all previously described loss-of-function mutations in laminin α2. Together, these new results argue strongly that the muscular dystrophy and amyelination resulting from laminin α2 mutations are not a simple derivative of the extent to which the BL is compromised or levels of laminin 2 are reduced. This conclusion is fully consistent with a previous study of laminins in myelination that found that BL integrity, per se, has little or no role (Yang et al., 2005). However, it differs from previous views regarding laminin-deficient muscular dystrophy.

The mechanisms leading to dystrophy in *nmf417* homozygotes probably encompass much of the pathogenic mechanism in *dy*^{2J} homozygotes. Dystrophy in *nmf417* and *dy*^{2J} homozygotes are remarkably similar in onset, progression and severity. C79, which is disrupted in *nmf417*, is included in the 57-residue deletion caused by the *dy*^{2J} mutation (Sunada et al., 1995; Xu et al., 1994b). However, the *dy*^{2J} deletion generates an array of molecular abnormalities, including decreased α2 protein levels and disrupted basal laminae, which obscures the relative contribution of each to the phenotype. *Nmf417* is therefore remarkable for its phenotypic severity despite its molecular normality.

Because BL stability and levels of laminin 2 are not decreased in *nmf417*-mutant muscle, we infer that the highly conserved CxxC motif is involved in a more specific molecular interaction that is crucial for proper laminin α2 function. Candidate interactions include binding of heparan sulfate or integrins on the cell surface, activities that have been mapped to the LN domain in previous studies (e.g. Ettner et al., 1998). Alternatively, the CxxC motif might be required for proper higher-level organization of the laminin meshwork within the mature BL (Yurchenco, 1990; Yurchenco et al., 2004a). LN-domains are thought to scaffold BL assembly by forming tripartite interactions between the α, β and γ chains of neighboring laminin heterotrimers. The CxxC motif could selectively disrupt pairings within the tripartite complex, permitting the assembly of a BL with an abnormal lattice. This interpretation is consistent with the increased BL thickness we often observed on *nmf417* mutant myofibers. The *dy*^{2J} mutation, which decreases overall polymer stability and BL structure, might therefore reflect a more complete loss of tripartite-complex formation.

Distinguishing these possible mechanisms will require additional experiments to study laminin polymerization, and to identify LN-domain binding partners and how these are altered by the C79 disruption. Ideally, these studies could be combined with structural analyses to determine whether C79 is involved in disulfide crosslinking, in which case the dysfunction could arise from gross alteration in N-terminal conformation. Future studies in which the *nmf417* allele is used to investigate laminin 2 polymerization are also appealing for two reasons. First, we have shown that other polymerizing α chains (α1, α5) are not upregulated in *nmf417* homozygous mice to compensate for the mutation in α2. Indeed,

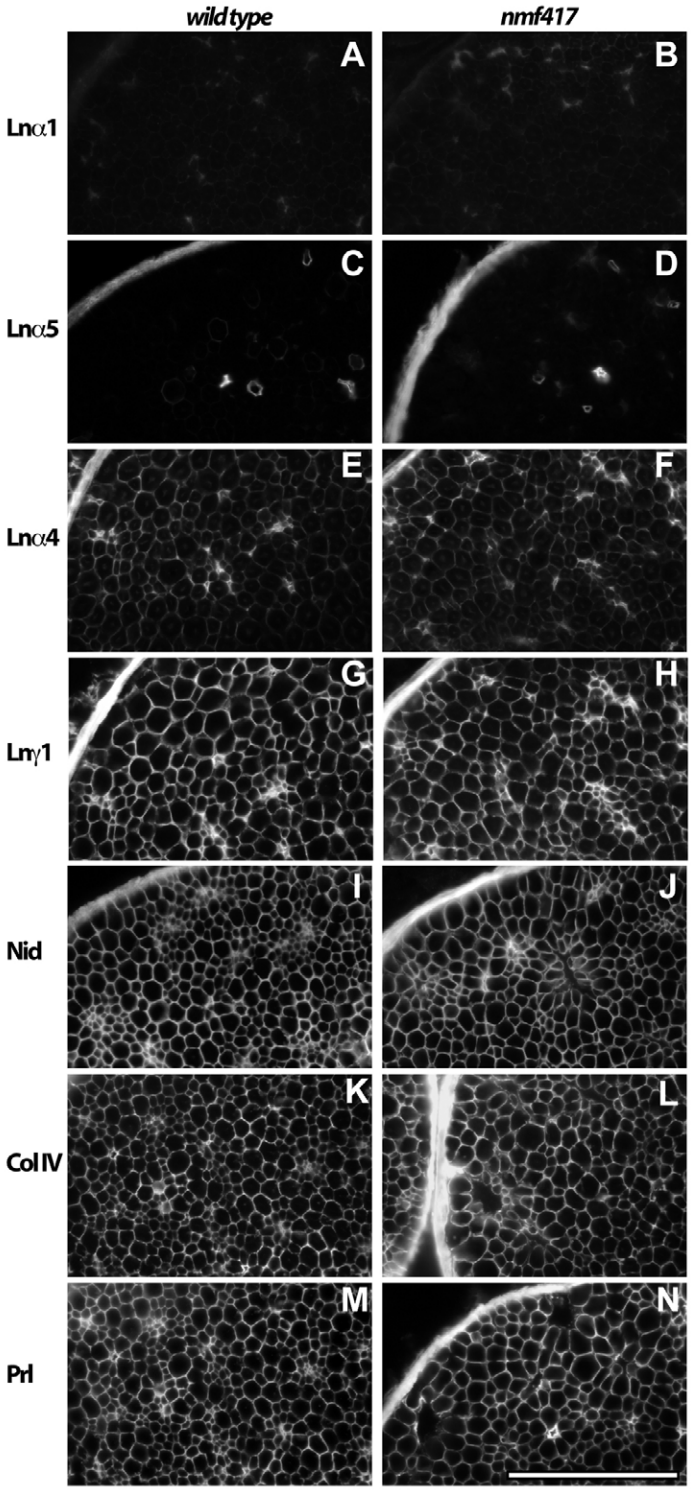

Fig. 7. Composition of Schwann cell BLs. Medial sciatic nerve sections from control and *nmf417*-mutant littermates were stained with antibodies against the indicated BL components. (A-D) Normal Schwann cells (A,C) produce little laminin (Ln) α1 and α5, and these were not upregulated in *nmf417* nerves (B,D). (E,F) Non-myelinating Schwann cells normally express high levels of laminin α4, whereas myelinating Schwann cells express α4 at low levels. There was no increase in α4 on myelinating Schwann cells in *nmf417* nerves. (G-N) The other primary components of endoneurial BLs, including laminin γ1 (G,H), nidogen (I,J), collagen IV (K,L) and perlecan (M,N), were also present at comparable levels and with normal localization in the mutant nerves. Scale bar: 60 μm.

α1 can substitute for α2 to prevent dystrophy and improve peripheral myelination, suggesting that the phenotype results from general laminin interactions or activities such as polymerization in the BL rather than activities that are specific to α2 (Gawlik et al., 2004; Gawlik et al., 2006). Second, the non-polymerizing α4 chain, which does not contain an N-terminal extension and LN domain, is also not upregulated. This aspect of *nmf417* is unique among mouse and human *Lama2* mutations (Patton et al., 1999). The lack of α4 upregulation is significant for interpreting polymerization studies because laminin 8 (α4β1γ1) might actually inhibit laminin polymerization in places where it is colocalized with laminin 2, when laminin 2 function is compromised. This competitive relationship is suggested by previous studies of laminins in myelination (Yang et al., 2005), and by the present study, in which we showed an absence of BL surrounding immature non-myelinating Schwann cells that express α4. At NMJs, another site of α4 localization, a BL still forms in mice homozygous for other *Lama2* alleles examined (Gilbert et al., 1973; Law et al., 1983; Patton et al., 2001), but this is presumably owing to the presence in the synaptic BL of α5, which serves as an alternative polymerizing α chain (Miner et al., 1997).

Mechanical properties of the BL, such as torsional flexibility or elasticity, might also be lost in *nmf417*. Such properties might relate to either laminin polymerization or other molecular interactions between BL components or between the BL and cell surface (Yurchenco et al., 2004b). A function for laminin 2 in maintaining sarcolemmal integrity during mechanical stress is attractive, and is consistent with mutations in other DGC genes that also cause dystrophy. However, *Lama2* mutations reportedly do not cause consistent sarcolemmal-integrity defects, as assayed by uptake of the azo-dye Evan's Blue, although scattered positive fibers are present in muscles and vary with age and severity of the allele studies (Straub et al., 1997) (B.L.P. and R.W.B., unpublished observations). Furthermore, a function in mechanical stabilization is more plausible in a contracting muscle than in the myelination of nerves during development. The failure of myelination is a consistent feature in human MDC1A and *Lama2*-mutant mice, but is not seen in most other dystrophy-causing mutations. Laminin 2 might be playing distinct roles in nerve and muscle BLs, but it is interesting that both of these functions would still depend on C79 and the LN domain of α2.

Nmf417 also offers several points of relevance for human MDC1A. First, loss-of-function *LAMA2* mutation can occur without loss of α2 protein. Some forms of MDC1A might therefore be misdiagnosed by immunocytochemistry, and ultimately require analysis of the entire *LAMA2* coding sequence for their correct diagnosis. Second, *nmf417* represents a reference for point mutations that perturb specific domain functions, without overall loss of expression or BL integrity. Several human *LAMA2* point mutations cause MDC1A, including L2564P, C862R and C527Y (He et al., 2001; Tezak et al., 2003), although none are in the LN domain. Third, *nmf417* might prove particularly useful in defining the unique contribution of laminin 2 to myelination. It will also be of great interest to determine whether defects in CNS myelination in human MDC1A and in dy^{2J} mice are replicated in *nmf417*. Finally, *nmf417* offers advantages over dy^{2J} as an experimental model. Mutant mice are readily genotyped as pups and can be

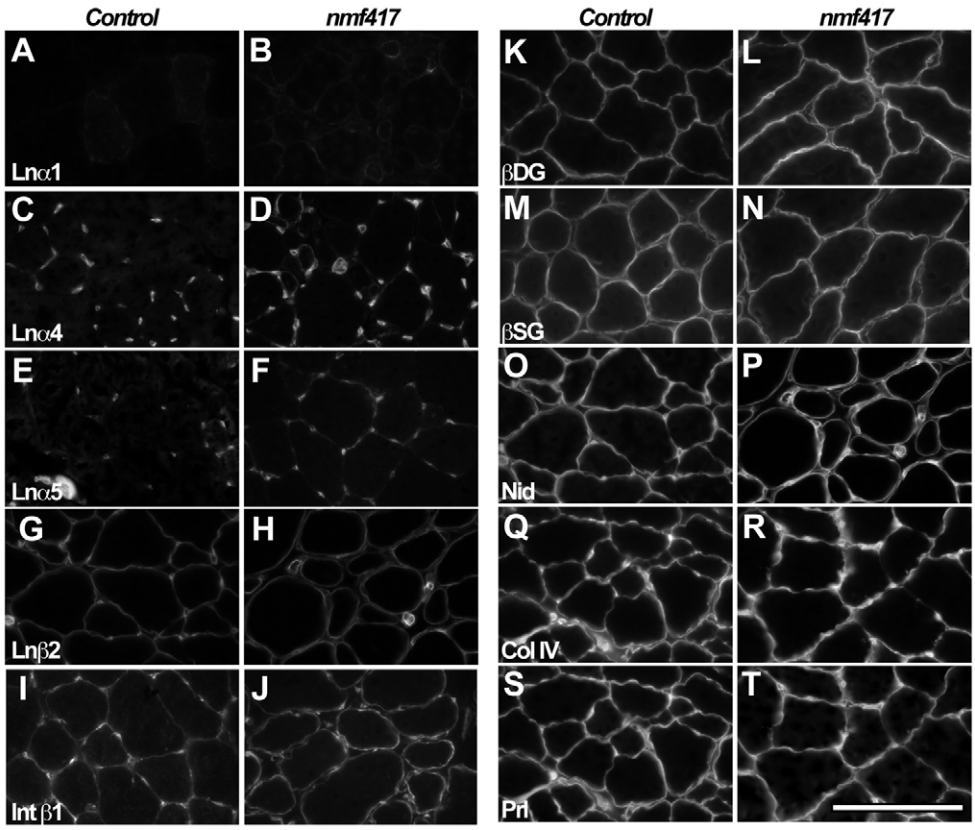

Fig. 8. Composition of muscle BLs. (A-T) Cross-sections of quadriceps from P59 *nmf417* and littermate controls were immunostained with antibodies against the indicated proteins and imaged with identical settings. Normal muscle fiber BL was rich in nidogen-1, collagen IV and perlecan, and contained low levels of laminin β2, but contained little or no laminin α1, α4 or α5. Laminins α4, α5 and β2 were concentrated in blood-vessel and perineurial BLs. Cell-surface proteins interacting with laminins were also examined, including β1 integrin, and β-sarcoglycan (βSG) and β-dystroglycan (βDG) were used as indicators of the DGC in muscle. There was little change in BL composition or cell-surface proteins in *nmf417*-mutant muscle. Notably, laminin α4 immunoreactivity increased on a subset of small-diameter fibers, but was absent from the majority of *nmf417* myofibers. Scale bar: 60 μm.

bred as homozygotes, produce a defined mutant protein and present with consistent phenotypic severity, all of which favor a reliable platform for interpreting therapeutic strategies.

Therefore, although many questions remain unanswered, we suggest that the phenotype of the *nmf417* allele indicates a crucial function for the LN domain, and more specifically the conserved C79, in laminin biology. Furthermore, *nmf417* mice provide an in vivo model for these studies without confounding issues such as decreased protein levels or the upregulation of other laminin α chains. Thus, the *nmf417* allele is a useful and convenient experimental model of MDC1A, which suggests new mechanistic relationships between BL formation, muscle fiber stability and Schwann cell differentiation.

Materials and Methods

Mouse nomenclature

The mice referred to in this study have the following official nomenclature: *nmf417* is *Lama2*$^{dy\text{-}7J}$; *dy*^{2J} is *Lama2*$^{dy\text{-}2J}$; *dy* is *Lama2*^{dy}; *dy*^{W} is *Lama2*^{tm1Eeng}; and *dy*^{3K} is *Lama2*^{tm1Stk}. All mice used were in a C57BL/6J genetic background, except *dy*, which were on a mix of C57BL/6 and 129P1/Re.

Mice

The *nmf417* allele was generated in a mutagenesis screen for recessive neurological mutations. Male C57BL/6J (B6) mice were mutagenized using ENU, allowed to recover fertility and bred to B6 females. Male offspring in generation 1 (G1), each carrying a unique assortment of mutations, were mated to B6 females to generate G2 females, which were bred back to the G1 male ancestor, producing homozygous recessive mutations in G3. G3 offspring were screened for neurological phenotypes using a battery of behavioral, clinical and histological analyses. The *nmf417* strain was initially identified based on overt hind-limb wasting and dysfunction, followed by histological characterization revealing skeletal muscular dystrophy and peripheral hypomyelination, and complementation with a known *Lama2*^{dy} allele heterozygote.

All mice were housed in PIV caging on a 12/12-hour light/dark cycle, and provided with food and water ad libidum. Protocols and procedures were designed in accordance with the Guide for the Care and Use of Laboratory Animals, and approved by the Animal Care and Use Committees of The Jackson Laboratory and Oregon Health Science University. Numbers and ages of mice used for each experiment are stated throughout the text.

Sequencing

Trizol (Invitrogen) was used according to the manufacturer's instructions to prepare total RNA from the brains of a B6 control, a known *nmf417* heterozygote and an affected (presumed homozygote) *nmf417* mouse. 5 μg total RNA was reverse transcribed to first-strand cDNA using Superscript III reverse transcriptase (Invitrogen) and a mix of oligo-dT and random primers. The *Lama2* coding sequence was amplified by PCR in 12 overlapping reactions of approximately 800 bp each, and the products sequenced directly on both strands and compared to sequence from the mouse genome project (www.Ensembl.org) and from isogenic control mice using the Sequencher analysis program.

Genotyping

The *nmf417* allele was genotyped using a PCR primer-mismatch assay in which a common reverse primer to *Lama2* intron2 is paired with wild-type and mutant forward primers in which the single mutated base is the second-to-last (penultimate) nucleotide. Primer sequences: *nmf417* F Wild-Type, 5′-CTGTGAGGAACCCTCAGTG-3′; *nmf417* F Mutant, 5′-CTGTGAGGAACCCTCAGCG-3′; *nmf417* R Intron2, 5′-CATTTCAGGACCTGTGTTGA-3′. Reaction conditions, using HotMaster Taq Polymerase (Eppendorf): wild-type specific reaction, 95°C for 5 minutes; 95°C for 25 seconds, 62°C for 35 seconds, 72°C for 45 seconds, for 30 cycles, and 72°C for 5 minutes; mutant specific reaction, 95°C for 5 minutes; 95°C for 25 seconds, 64°C for 35 seconds, 72°C for 45 seconds, for 38 cycles, and 72°C for 5 minutes.

Antibodies

Sources for primary antibodies were: laminin α1 mAb-198, provided by L. Sorokin (University of Münster, Germany); laminin α2 mAb 4H8-2 from Alexis Pharmaceuticals (San Diego, CA); affinity purified rabbit polyclonal Abs to the α2 G-domains provided by Peter Yurchenco (Robert Wood Johnson Medical School, Piscataway, NJ) and Takako Sasaki (#1078+E; Shriners Hospital, Portland, OR); laminin β1 (MAB1928), laminin γ1 (MAB1914), nidogen-1 (MAB1946), perlecan (MAB1948) and collagen IV (AB756P) all from Chemicon (Temecula, CA); rabbit antibodies to laminin α5 (1113+) and γ3 (1138+) from T. Sasaki (OHSU, Portland, OR); rabbit laminin 5 antisera (including the α3, β3 and γ2 chains, from M. P.

Marinkovich (Stanford University, Palo Alto, CA); affinity-purified rabbit antibodies to agrin from M. Ferns (McGill University, Montreal, Quebec) and D. Glass (Regeneron, Tarrytown, NJ). Additional antisera to laminin β2, α4 and α5 are described (Miner et al., 1997). Alexa-fluorochrome-conjugated second antibodies were from Molecular Probes (Eugene, OR).

Histology and electron microscopy

For histology, muscles were dissected free, immersed using Bouin's fixative, embedded in paraffin, microtome sectioned at 5 μm and stained using Hemotoxylin and Eosin (H&E) by standard protocols. Nerve tissue was dissected free; fixed in 2% glutaraldehyde, 2% paraformaldehyde in 0.1 M cacodylate; post-fixed in 1% OsO_4; embedded in plastic; sectioned at 0.5 μm; and stained with Toluidine Blue for light microscopy. For TEM, 50- to 100-nm plastic sections of nerve and muscle were examined on a Jeol 1230 80 kV electron microscope and imaged with a Hamamatsu digital camera. For immunohistochemistry, unfixed tissues were flash frozen in liquid-N_2 cooled freezing compound and cryosectioned at 8 μm. Prior to freezing, normal and mutant nerves were sandwiched in parallel between pieces of diaphragm, to ensure identical processing.

Western blotting

Muscle extracellular matrix fractions were prepared similar to methods previously described for kidney (Miner et al., 1997). Tissue was homogenized at 0-4°C in five volumes of low-ionic-strength buffer containing protease inhibitors. A crude membrane fraction (30 minutes at 30,000 ***g***) was washed once, resuspended in three volumes of buffer, supplemented with 1.0 M NaCl and 1% Triton X-100 and sonicated 90 seconds, and centrifuged for 30 minutes at 100,000 ***g***. Protein content of matrix-rich insoluble pellets was determined by a detergent-compatible Lowry assay (Peterson, 1977) with BSA as standard. Samples of control and *nmf417* matrix fractions containing equal protein content were heated in SDS sample buffer without reducing agents, loaded into neighboring slot wells (5 μg/mm) of Laemmli polyacrylamide gel, and separated as described (Miner et al., 1997). Nitrocellulose transfers were blocked with Tween-20 and parallel strips were cut from each sample area, numbered and incubated overnight in a single set of diluted antibodies. Reducing westerns for α2 quantification were performed as above, except that tissue homogenates were used to avoid potential differences in matrix stability; 100 mM DTT was added to the gel sample buffer. Equal amounts of total protein were loaded and blots were probed with antibodies against α2 (pAb 1078+E), and the same blots were reprobed with an antibody against myosin heavy chain, which served as a normalization control for sample loading. Bound antibodies were detected with HRP-conjugated second antibodies, chemiluminescent substrate (Supersignal WestFemto, Pierce, Rockford, IL) and Kodak X-OMAT film.

Statistical analysis

All statistical comparisons were done using two-tailed *t*-tests and a significance threshold of $P<0.05$ was used.

We thank Takako Sasaki, Lydia Sorokin and Peter Yurchenco for generously providing antibodies; Kate Miers, Steve Rauch, Joel Gay and Janis McFerrin for technical assistance; Gregory Cox for comments on the manuscript; and Pete Finger and the Histology and Microscopy service at The Jackson Laboratory, which is supported by the NCI Cancer Center (CA034196). Work was supported by grants from the Muscular Dystrophy Association and NIH (NS040759) to B.L.P. and by NIH (UO1-NS41215) for the mutagenesis program at The Jackson Laboratory.

References

Aumailley, M., Bruckner-Tuderman, L., Carter, W. G., Deutzmann, R., Edgar, D., Ekblom, P., Engel, J., Engvall, E., Hohenester, E., Jones, J. C. et al. (2005). A simplified laminin nomenclature. *Matrix Biol.* **24**, 326-332.

Benninger, Y., Thurnherr, T., Pereira, J. A., Krause, S., Wu, X., Chrostek-Grashoff, A., Herzog, D., Nave, K. A., Franklin, R. J., Meijer, D. et al. (2007). Essential and distinct roles for cdc42 and rac1 in the regulation of Schwann cell biology during peripheral nervous system development. *J. Cell Biol.* **177**, 1051-1061.

Biscoe, T. J., Caddy, K. W., Pallot, D. J. and Pehrson, U. M. (1975). Investigation of cranial and other nerves in the mouse with muscular dystrophy. *J. Neurol. Neurosurg. Psychiatr.* **38**, 391-403.

Bradley, W. G. and Jenkison, M. (1973). Abnormalities of peripheral nerves in murine muscular dystrophy. *J. Neurol. Sci.* **18**, 227-247.

Bradley, W. G. and Jenkison, M. (1975). Neural abnormalities in the dystrophic mouse. *J. Neurol. Sci.* **25**, 249-255.

Bunge, R. P., Bunge, M. B. and Eldridge, C. F. (1986). Linkage between axonal ensheathment and basal lamina production by Schwann cells. *Annu. Rev. Neurosci.* **9**, 305-328.

Cheng, Y. S., Champliaud, M. F., Burgeson, R. E., Marinkovich, M. P. and Yurchenco, P. D. (1997). Self-assembly of laminin isoforms. *J. Biol. Chem.* **272**, 31525-31532.

Cohn, R. D., Herrmann, R., Sorokin, L., Wewer, U. M. and Voit, T. (1998). Laminin alpha2 chain-deficient congenital muscular dystrophy: variable epitope expression in severe and mild cases. *Neurology* **51**, 94-100.

Colognato, H. and Yurchenco, P. D. (1999). The laminin alpha2 expressed by dystrophic dy(2J) mice is defective in its ability to form polymers. *Curr. Biol.* **9**, 1327-1330.

Colognato, H. and Yurchenco, P. D. (2000). Form and function: the laminin family of heterotrimers. *Dev. Dyn.* **218**, 213-234.

Ettner, N., Gohring, W., Sasaki, T., Mann, K. and Timpl, R. (1998). The N-terminal globular domain of the laminin alpha1 chain binds to alpha1beta1 and alpha2beta1 integrins and to the heparan sulfate-containing domains of perlecan. *FEBS Lett.* **430**, 217-221.

Gawlik, K., Miyagoe-Suzuki, Y., Ekblom, P., Takeda, S. and Durbeej, M. (2004). Laminin alpha1 chain reduces muscular dystrophy in laminin alpha2 chain deficient mice. *Hum. Mol. Genet.* **13**, 1775-1784.

Gawlik, K. I., Li, J. Y., Petersen, A. and Durbeej, M. (2006). Laminin alpha1 chain improves laminin alpha2 chain deficient peripheral neuropathy. *Hum. Mol. Genet.* **15**, 2690-2700.

Gilbert, J. J., Steinberg, M. C. and Banker, B. Q. (1973). Ultrastructural alterations of the motor end plate in myotonic dystrophy of the mouse (dy2J dy2J). *J. Neuropathol. Exp. Neurol.* **32**, 345-364.

He, Y., Jones, K. J., Vignier, N., Morgan, G., Chevallay, M., Barois, A., Estournet-Mathiaud, B., Hori, H., Mizuta, T., Tome, F. M. et al. (2001). Congenital muscular dystrophy with primary partial laminin alpha2 chain deficiency: molecular study. *Neurology* **57**, 1319-1322.

Kuang, W., Xu, H., Vachon, P. H., Liu, L., Loechel, F., Wewer, U. M. and Engvall, E. (1998). Merosin-deficient congenital muscular dystrophy. Partial genetic correction in two mouse models. *J. Clin. Invest.* **102**, 844-852.

Law, P. K., Saito, A. and Fleischer, S. (1983). Ultrastructural changes in muscle and motor end-plate of the dystrophic mouse. *Exp. Neurol.* **82**, 404-412.

Leivo, I. and Engvall, E. (1988). Merosin, a protein specific for basement membranes of Schwann cells, striated muscle, and trophoblast, is expressed late in nerve and muscle development. *Proc. Natl. Acad. Sci. USA* **85**, 1544-1548.

Madrid, R. E., Jaros, E., Cullen, M. J. and Bradley, W. G. (1975). Genetically determined defect of Schwann cell basement membrane in dystrophic mouse. *Nature* **257**, 319-321.

Michelson, A. M., Russell, E. S. and Harman, P. J. (1955). Dystrophia muscularis: a hereditary primary myopathy in the house mouse. *Proc. Natl. Acad. Sci. USA* **12**, 1079-1084.

Miner, J. H., Patton, B. L., Lentz, S. I., Gilbert, D. J., Snider, W. D., Jenkins, N. A., Copeland, N. G. and Sanes, J. R. (1997). The laminin alpha chains: expression, developmental transitions, and chromosomal locations of alpha1-5, identification of heterotrimeric laminins 8-11, and cloning of a novel alpha3 isoform. *J. Cell Biol.* **137**, 685-701.

Miyagoe, Y., Hanaoka, K., Nonaka, I., Hayasaka, M., Nabeshima, Y., Arahata, K. and Takeda, S. (1997). Laminin alpha2 chain-null mutant mice by targeted disruption of the Lama2 gene: a new model of merosin (laminin 2)-deficient congenital muscular dystrophy. *FEBS Lett.* **415**, 33-39.

Moll, J., Barzaghi, P., Lin, S., Bezakova, G., Lochmuller, H., Engvall, E., Muller, U. and Ruegg, M. A. (2001). An agrin minigene rescues dystrophic symptoms in a mouse model for congenital muscular dystrophy. *Nature* **413**, 302-307.

Nakagawa, M., Miyagoe-Suzuki, Y., Ikezoe, K., Miyata, Y., Nonaka, I., Harii, K. and Takeda, S. (2001). Schwann cell myelination occurred without basal lamina formation in laminin alpha2 chain-null mutant (dy3K/dy3K) mice. *Glia* **35**, 101-110.

Nodari, A., Zambroni, D., Quattrini, A., Court, F. A., D'Urso, A., Recchia, A., Tybulewicz, V. L., Wrabetz, L. and Feltri, M. L. (2007). Beta1 integrin activates Rac1 in Schwann cells to generate radial lamellae during axonal sorting and myelination. *J. Cell Biol.* **177**, 1063-1075.

Patton, B. L., Miner, J. H., Chiu, A. Y. and Sanes, J. R. (1997). Distribution and function of laminins in the neuromuscular system of developing, adult, and mutant mice. *J. Cell Biol.* **139**, 1507-1521.

Patton, B. L., Connoll, A. M., Martin, P. T., Cunningham, J. M., Mehta, S., Pestronk, A., Miner, J. H. and Sanes, J. R. (1999). Distribution of ten laminin chains in dystrophic and regenerating muscles. *Neuromuscul. Disord.* **9**, 423-433.

Patton, B. L., Cunningham, J. M., Thyboll, J., Kortesmaa, J., Westerblad, H., Edstrom, L., Tryggvason, K. and Sanes, J. R. (2001). Properly formed but improperly localized synaptic specializations in the absence of laminin alpha4. *Nat. Neurosci.* **4**, 597-604.

Peterson, G. L. (1977). A simplification of the protein assay method of Lowry et al. which is more generally applicable. *Anal. Biochem.* **83**, 346-356.

Previtali, S. C., Dina, G., Nodari, A., Fasolini, M., Wrabetz, L., Mayer, U., Feltri, M. L. and Quattrini, A. (2003). Schwann cells synthesize alpha7beta1 integrin which is dispensable for peripheral nerve development and myelination. *Mol. Cell. Neurosci.* **23**, 210-218.

Ringelmann, B., Roder, C., Hallmann, R., Maley, M., Davies, M., Grounds, M. and Sorokin, L. (1999). Expression of laminin alpha1, alpha2, alpha4, and alpha5 chains, fibronectin, and tenascin-C in skeletal muscle of dystrophic 129ReJ dy/dy mice. *Exp. Cell Res.* **246**, 165-182.

Sanes, J. R., Engvall, E., Butkowski, R. and Hunter, D. D. (1990). Molecular heterogeneity of basal laminae: isoforms of laminin and collagen IV at the neuromuscular junction and elsewhere. *J. Cell Biol.* **111**, 1685-1699.

Sasaki, T., Fassler, R. and Hohenester, E. (2004). Laminin: the crux of basement membrane assembly. *J. Cell Biol.* **164**, 959-963.

Sewry, C. A., Naom, I., D'Alessandro, M., Sorokin, L., Bruno, S., Wilson, L. A., Dubowitz, V. and Muntoni, F. (1997). Variable clinical phenotype in merosin-deficient

congenital muscular dystrophy associated with differential immunolabelling of two fragments of the laminin alpha 2 chain. *Neuromuscul. Disord.* **7**, 169-175.

Sewry, C. A., Uziyel, Y., Torelli, S., Buchanan, S., Sorokin, L., Cohen, J. and Watt, D. J. (1998). Differential labelling of laminin alpha 2 in muscle and neural tissue of dy/dy mice: are there isoforms of the laminin alpha 2 chain? *Neuropathol. Appl. Neurobiol.* **24**, 66-72.

Shelton, G. D. and Engvall, E. (2005). Canine and feline models of human inherited muscle diseases. *Neuromuscul. Disord.* **15**, 127-138.

Straub, V. and Campbell, K. P. (1997). Muscular dystrophies and the dystrophin-glycoprotein complex. *Curr. Opin. Neurol.* **10**, 168-175.

Straub, V., Rafael, J. A., Chamberlain, J. S. and Campbell, K. P. (1997). Animal models for muscular dystrophy show different patterns of sarcolemmal disruption. *J. Cell Biol.* **139**, 375-385.

Sunada, Y., Bernier, S. M., Kozak, C. A., Yamada, Y. and Campbell, K. P. (1994). Deficiency of merosin in dystrophic dy mice and genetic linkage of laminin M chain gene to dy locus. *J. Biol. Chem.* **269**, 13729-13732.

Sunada, Y., Bernier, S. M., Utani, A., Yamada, Y. and Campbell, K. P. (1995). Identification of a novel mutant transcript of laminin alpha 2 chain gene responsible for muscular dystrophy and dysmyelination in dy2J mice. *Hum. Mol. Genet.* **4**, 1055-1061.

Tezak, Z., Prandini, P., Boscaro, M., Marin, A., Devaney, J., Marino, M., Fanin, M., Trevisan, C. P., Park, J., Tyson, W. et al. (2003). Clinical and molecular study in congenital muscular dystrophy with partial laminin alpha 2 (LAMA2) deficiency. *Hum. Mutat.* **21**, 103-111.

Tome, F. M., Evangelista, T., Leclerc, A., Sunada, Y., Manole, E., Estournet, B., Barois, A., Campbell, K. P. and Fardeau, M. (1994). Congenital muscular dystrophy with merosin deficiency. *C. R. Acad. Sci. III* **317**, 351-357.

Weinberg, H. J., Spencer, P. S. and Raine, C. S. (1975). Aberrant PNS development in dystrophic mice. *Brain Res.* **88**, 532-537.

Xu, H., Christmas, P., Wu, X. R., Wewer, U. M. and Engvall, E. (1994a). Defective muscle basement membrane and lack of M-laminin in the dystrophic dy/dy mouse. *Proc. Natl. Acad. Sci. USA* **91**, 5572-5576.

Xu, H., Wu, X. R., Wewer, U. M. and Engvall, E. (1994b). Murine muscular dystrophy caused by a mutation in the laminin alpha 2 (Lama2) gene. *Nat. Genet.* **8**, 297-302.

Yang, D., Bierman, J., Tarumi, Y. S., Zhong, Y. P., Rangwala, R., Proctor, T. M., Miyagoe-Suzuki, Y., Takeda, S., Miner, J. H., Sherman, L. S. et al. (2005). Coordinate control of axon defasciculation and myelination by laminin-2 and -8. *J. Cell Biol.* **168**, 655-666.

Yurchenco, P. D. (1990). Assembly of basement membranes. *Ann. N. Y. Acad. Sci.* **580**, 195-213.

Yurchenco, P. D., Amenta, P. S. and Patton, B. L. (2004a). Basement membrane assembly, stability and activities observed through a developmental lens. *Matrix Biol.* **22**, 521-538.

Yurchenco, P. D., Cheng, Y. S., Campbell, K. and Li, S. (2004b). Loss of basement membrane, receptor and cytoskeletal lattices in a laminin-deficient muscular dystrophy. *J. Cell Sci.* **117**, 735-742.